

# Dynamical interplay between local connectivity and global competition in a networked population

S. Gourley<sup>1</sup>, S.C. Choe<sup>1</sup>, P.M. Hui<sup>2</sup>, and N.F. Johnson<sup>1</sup>

<sup>1</sup> Clarendon Laboratory, Physics Department, Oxford University, Oxford OX1 3NP, United Kingdom,

<sup>2</sup> Department of Physics, The Chinese University of Hong Kong, Shatin, New Territories, Hong Kong  
(July 23, 2019)

We show, both numerically and analytically, that the consequences of ‘wiring up’ a competitive population depend quite dramatically on the interplay between the local connectivity and the global resources. With modest global resources, adding small amounts of local connectivity yields an increasingly heterogeneous population. With substantial global resources, high-performing yet reasonably homogenous collective states emerge instead.

PACS numbers: 02.50.Le, 87.23.Kg, 89.65.Ef, 05.40.2a

Is ‘getting connected’ a good or bad thing? How does increased access to both global (i.e. public) information *and* local (i.e. private) information, affect both the population as a whole and its individual members? Thinking in terms of future technologies, what are the possible benefits and dangers of introducing communication channels between collections of intelligent devices, microsensors, semi-autonomous robots, nanocomputers, and even biological micro-organisms such as bacteria [1,2]? These questions are relevant to a wide range of computational, technological, biological and socio-economic systems. However such questions are very difficult to answer since these systems are simply ‘too complex’ [3–7].

Here we examine these questions using a minimal generic model which mimics a group of selfish, rational individuals or components, referred to simply as ‘agents’. These agents repeatedly compete for a global resource by making inductive decisions about future group behavior. The population and its agents may be biological (e.g. a population of cellular organisms competing for nutrients), computational (e.g. a grid of software modules competing for processing time), mechanical (e.g. a constellation of sensors or devices competing for communications bandwidth or operating power) or social (e.g. a population of companies competing for business). We uncover a rich interplay between the global competition for resources and the local inter-agent connectivity. In a population with modest resources, low levels of inter-connectivity increase the disparity between successful and unsuccessful agents. By contrast in a higher-resource population with low inter-connectivity, high-performing collective states can spontaneously arise in which nearly all agents are reasonably successful. At high levels of inter-connectivity, the overall population becomes fairer (i.e. smaller spread in success-rates) but less efficient (i.e. smaller mean success-rate) irrespective of the global resource level.

Our B-A-R (Binary Agent Resource) model is a minimal generic model of a competitive networked population, which is based on Arthur’s so-called El Farol Problem [4] in which a population of agents repeatedly com-

pete for a limited resource (i.e. seating in a crowded bar) [8]. Despite its everyday human setting, the El Farol Problem embodies key generic characteristics of Complex Systems [4,2]: feedback and adaptation at the macroscopic and/or microscopic level, many interacting parts, non-stationarity, evolution, coupling with the environment, and observed dynamics which depend upon the particular realization of the system. Although the El Farol Problem is more general than, say, the Minority Game [5,2,6] in that it allows for arbitrary levels of global resource and is non-binary, the agents still only have access to *global* information. Most biological, informational and socio-economic systems have at least some degree of underlying connectivity among agents [2] leading to exchange of *local* information. It is the resulting interplay of network connectivity and competition for global resources that we wish to explore and understand. Therefore in contrast to previous works [4–6,2] our B-A-R model features network connectivity *and* a general global resource level  $L$ . Here  $L$ , which is not announced to the agents, may represent the optimal load capacity of a regional power grid, public utility, or electronic microcircuit; the available space in a given urban region, public area or popular bar; the data capacity of a given communications link in an informational or biological system; the vehicular or passenger capacity on a given road or transport system.

At each timestep  $t$ , each agent decides whether to access resource  $L$  (i.e. action +1 which might correspond to an electronic component or device deciding to draw power, a computer sending a data-packet down a given route, a surfer accessing a particular website, a commuter taking a given road to work) or not to access this resource (i.e. action –1). The two global outcomes at each timestep, ‘resource over-used’ and ‘resource not over-used’, are denoted as ‘0’ and ‘1’. If the number of agents  $n_{+1}[t]$  choosing action +1 exceeds  $L$  (i.e. resource over-used and hence global outcome ‘0’) then the  $n_{-1}[t]$  abstaining agents win. By contrast if  $n_{+1}[t] \leq L$  (i.e. resource not over-used and hence global outcome ‘1’) then these  $n_{+1}[t]$  agents win. Each agent decides its actions in light of (i) *global information* which takes the

form of the history of the  $m$  most recent global outcomes, and (ii) *local information* obtained via network connections. Adaptation is introduced by randomly assigning  $S$  strategies to each agent. Each of the  $2^m$  possible strategies is a bitstring of length  $2^m$  defining an action (+1 or -1) for each of the  $2^m$  possible global outcome histories. For example,  $m = 2$  has  $2^2 = 4$  possible global outcome histories: 00, 01, 10 and 11. Consequently there are  $2^{2^{m-2}} = 16$  possible strategies. Strategies which predicted the winning (losing) action at a given timestep, are assigned (deducted) one point. At each timestep, each agent compares the score of his own best-scoring strategy (or strategies) with the highest-scoring strategy (or strategies) among the agents to whom he is connected. The agent adopts the action of whichever strategy is highest-scoring overall, using a coin-toss to break any ties. For simplicity we here assume a random network, where the connection between any two agents exists with a probability  $p$ . We emphasize that *any* of the above model assumptions can easily be generalized: the numerical results are reasonably robust.

Figure 1 shows the mean success-rate per agent, averaged over many numerical realizations of the underlying connections and strategy distributions (left axis: solid curve) and the success-rate distribution within the population for a typical run (right axis: histograms) as a function of the inter-connectivity  $p$  in a modest-resource population. We have chosen  $L = (N - 1)/2$ , which is representative of modest resources since there are more losers than winners. We focus on the small  $m$  or ‘crowded’ regime [5,7,8] since there are relatively few strategies compared to the number of agents and hence many agents will simultaneously be competing to win with the same strategy. The mean success-rate decreases rapidly as  $p$  increases (left axis: solid curve) before saturating at  $p = p_{sat} \sim 0.1$ . As  $m$  increases,  $p_{sat}$  increases – full results for the uncrowded, large  $m$  regime will be discussed elsewhere. The success-rate distribution for a typical run (right axis: histogram) at  $p = 0$  exhibits a definite ‘class structure’ in terms of success. Dramatic changes then arise as  $p$  increases. The spread in the success-rate – shown explicitly in the inset and by vertical arrows in Fig. 1 – indicates a rapid increase in the population’s heterogeneity in the range  $0 \leq p \leq 0.02$ . The success-rate distribution becomes almost continuous, washing out the  $p = 0$  class structure. Above  $p \sim 0.02$ , there is a rapid drop in the proportion of highly-successful agents. Further increasing  $p$  leads to a decrease of the spread in success-rates. High levels of inter-connectivity therefore provide increased fairness (i.e. small spread in success-rate) but decreased efficiency (i.e. small mean success-rate).

Figure 2 compares our analytical results using the Crowd-Anticrowd theory [7,8] to the numerical results for the mean success-rate per agent. As will be explained in more detail elsewhere, the mean success-rate per agent

can be obtained from the standard deviation of the number of agents making a given choice (e.g. +1), by averaging this quantity over the attractors of the system (i.e. averaging over the Eulerian Trail [9] or subsets of it). The mean success-rate can hence be expressed [7,8] in terms of the mean number or *Crowd* of agents using the  $K$ ’th highest-scoring strategy (i.e.  $n_K^{net}$ ) and the mean number or *Anticrowd* of agents using strategy  $\bar{K}$  which is anti-correlated to  $K$  (i.e.  $n_{\bar{K}}^{net}$  where  $\bar{K} = 2^{m+1} + 1 - K$ ). Explicitly

$$n_K^{net} = n_K + n_{\rightarrow K} - n_{K\rightarrow} \quad (1)$$

where  $n_K$  is the number of agents who would have used strategy  $K$  in the absence of the network because of the initial random strategy allocation:

$$n_K = N \left( \left[ 1 - \frac{(K-1)}{2^{m+1}} \right]^S - \left[ 1 - \frac{K}{2^{m+1}} \right]^S \right). \quad (2)$$

In short,  $n_K$  is the intrinsic Crowd-size due to crowding in the global strategy space.  $n_{\rightarrow K}$  is a sum over all agents who use strategy  $K$  as a direct result of a network connection:

$$n_{\rightarrow K} = \left[ \sum_{J>K} n_J \right] \left[ (1-p)^{\sum_{G<K} n_G} \right] \left[ 1 - (1-p)^{n_K} \right]. \quad (3)$$

Hence  $n_{\rightarrow K}$  represents the *increase* in Crowd-size due to the local connectivity. By contrast,  $n_{K\rightarrow}$  is a sum over all agents who would have used  $K$  in the absence of a network, but who will now use a better strategy as a result of their network connections:

$$n_{K\rightarrow} = n_K \left[ 1 - (1-p)^{\sum_{G<K} n_G} \right]. \quad (4)$$

Hence  $n_{K\rightarrow}$  represents the *decrease* in Crowd-size due to the local connectivity. The resulting analytic expressions for the mean success-rate are in excellent agreement with numerical results (see Fig. 2) implying that the population’s dynamical evolution is indeed governed by crowds resulting from the interplay between *local* connectivity and *global* competition.

Figure 3 shows the mean success-rate per agent (thin solid lines) as a function of the inter-connectivity  $p$  in higher-resource populations, for a range of  $L$  values and small  $m$ . If the global resource level  $L$  exceeds a critical amount  $L_{crit} = 3N/4$ , the mean success-rate per agent can exhibit a *maximum* at small but finite inter-connectivity, for the following reason. When  $L > L_{crit}$  and  $p = 0$ , the population inhabits a ‘frozen’ state in the sense that the global outcome is persistently 1, i.e. ...111111. With  $S = 2$  as in Fig. 3, each agent has probability 1/4 of being assigned two strategies which both

define action  $-1$  following a string of  $m$  '1's. Thus approximately  $1/4$  of the population always lose and  $3/4$  of the population always win, leading to  $L_{crit} = 3N/4 \approx 75$ . The global resource is therefore under-used at  $p = 0$  by  $\Delta L \approx (L - 3N/4)$  at each timestep. Therefore increasing  $p$  away from  $p = 0$  will benefit some of the less successful agents by connecting them up to successful agents, thereby giving them access to  $\Delta L$ , until a  $p$  value is reached where the connectivity is sufficient to break the outcome series of 1's. These run-averaged results can be better understood by considering run-specific results for  $L = 100$  as an illustrative case (scattered circles). Specific runs appear to aggregate into groups having similar temporal dynamics and success-rate distributions – these groups correspond to different dynamical states of the system. The increase in the mean success-rate at low  $p$ , corresponds to the system following an *Efficient* State E which has an outcome series of 1's as discussed above. The success-rate distribution in State E (inset) is characterized by groups of persistent winners and losers. As  $p$  increases further, the outcome series for high  $L$  tends to move through a set of Intermediate States which combine a low spread in success-rate with a high mean (e.g. Intermediate States A and B). In Intermediate State A, the least-successful agents (which in State E had zero success) now have a success-rate which *exceeds* the average success-rate in the high connectivity limit. In the high  $p$  limit, the outcome series tends toward the period-4 Eulerian Trail [9] given by  $\dots 00110011\dots$ . The corresponding number of agents taking action  $+1$  follows the pattern  $\dots N, N, N/2, N/2, N, N, N/2, N/2\dots$ . The resulting *Fair* State F corresponds to all agents having access to the best performing strategies, either by being assigned that strategy or by being connected to another agent with that strategy. The resulting system is fair but inefficient, having a small spread but also a small mean success-rate  $\approx 0.25$ .

Figure 4 shows the mean success-rate per agent (thin solid lines) as a function of the inter-connectivity  $p$  in a high-resource population ( $L = 95$ ) for various history bit-string lengths  $m$ . The Intermediate States, characterized by a reasonably high mean success-rate and a reasonably small spread (see Fig. 3 inset), have an increasingly dominant effect on the system's behavior as  $m$  increases. For a particular value of  $m$ , increasing  $p$  moves the system toward cycles of increasing period and hence the fractions of 1's and 0's in the output series become more equal. The resulting State F, which represents an increasingly noisy version of the Eulerian Trail as  $m$  increases, is fair but inefficient (see Fig. 3 inset).

We have derived analytic expressions (thick solid lines in Figs. 3 and 4) which describe well the three dynamical regimes exhibited by the numerical results. The upper analytic branch at low  $p$ , describing the efficient State E, is given by:

$$\frac{3}{4} + \frac{1}{4} \left[ 1 - (1-p)^{\frac{3N}{4}} \right]. \quad (5)$$

The middle analytic branch at intermediate  $p$ , describing the Intermediate States, is given by:

$$\frac{3}{4} - \frac{9}{32}(1-p)^{\frac{7N}{16}} - \frac{1}{32}(1-p)^{\frac{15N}{16}} + \frac{1}{8}(1-p)^{\frac{3N}{4}}. \quad (6)$$

The lower analytic branch at high  $p$ , describing the fair State F, is given by:

$$\frac{1}{4} + \frac{9}{128}(1-p)^{\frac{7N}{16}} + \frac{1}{128}(1-p)^{\frac{15N}{16}} + \frac{1}{16}(1-p)^{\frac{3N}{4}}. \quad (7)$$

The outcome series of 1's at low  $p$  which yield State E, can persist up to  $p_{crit} \sim 1 - (1 - 4\Delta L/N)^{4/3N}$ . For  $L = 80, 90, 95$  and  $100$ , this yields  $p_{crit} \sim 0.002, 0.011, 0.019$  and  $0.042$  respectively, which are also all in excellent agreement with the numerical results. A full analysis of the dynamics of, and switching between, these regimes will be given elsewhere.

In conclusion, we have reported a rich dynamical interplay between local connectivity and global competition in a generic networked population. Apart from the intrinsic interest regarding functionality in complex system networks, our results suggest that the internal connectivity and global resources in such systems can be engineered in order to enhance performance.

PMH acknowledges support from the Research Grants Council of the Hong Kong SAR Government (grant CUHK4241/01P).

- 
- [1] For microsensors, see the article *The smart-dust revolution*, in *The World in 2004* (The Economist, London, 2004) p. 141. For robots and nanobots, see T. Hogg, *Nanotechnology* **10**, 300 (1999). For nanostructure components, see D. Challet and N.F. Johnson, *Phys. Rev. Lett.* **89**, 028701 (2002).
  - [2] On-line proceedings of IMA 'Hot Topics' Workshop on Agent Based Modeling and Simulation (2003) at [www.ima.umn.edu/complex/fall/agent.html](http://www.ima.umn.edu/complex/fall/agent.html); International Workshop on Complex Agent-based Dynamic Networks (2003) at [sbs-xnet.sbs.ox.ac.uk/complexity/complexity\\_workshop\\_2003.asp](http://sbs-xnet.sbs.ox.ac.uk/complexity/complexity_workshop_2003.asp); Workshop on Collectives and the Design of Complex Systems (2003) at [collectives.stanford.edu/cdocs03/register.html](http://collectives.stanford.edu/cdocs03/register.html)
  - [3] J.E. Stiglitz, *Globalization and Its Discontents* (Penguin, London, 2002); A. Soulier and T. Halpin-Healy, *Phys. Rev. Lett.* **90**, 258103 (2003); E. Fehr, B. Rockenbach, *Nature* **422**, 137 (2003); R.V. Sole, B. Goodwin, *Sign of Life: How Complexity Pervades Biology* (Basic Books, New York, 2000); S.N. Dorogovtsev, J.F.F. Mendes, *Evolution of Networks: From Biological Nets to the Internet and WWW*

- (Oxford University Press, Oxford, 2002); D.J. Watts, S.H. Strogatz, *Nature* **393**, 440 (1998); B.A. Huberman, L.A. Adamic, *Nature* **401**, 131 (1999); A.-L. Barabási, R. Albert, H. Jeong, G. Bianconi, *Science* **287**, 2115 (2000); F. Liljeros, C.R. Edling, L.A. N. Amaral, H.E. Stanley, Y. Åberg, *Nature* **411**, 907 (2001); M.E.J. Newman, S.H. Strogatz, D.J. Watts, *Phys. Rev. E* **64**, 026118 (2001); P.S. Dodds, R. Muhamad, D.J. Watts, *Science* **301**, 827 (2003).
- [4] W.B. Arthur, *Science* **284**, 107 (1999); J.L. Casti, *Would-be Worlds* (Wiley, New York, 1997), p. 213.
- [5] D. Challet, Y.C. Zhang, *Physica A* **246** 407 (1997).
- [6] M. Anghel, Z. Toroczkai, K.E. Bassler, G. Kroniss, cond-mat/0307740; I. Caridi, H. Ceva, cond-mat/0401372.
- [7] M. Hart, P. Jefferies, N. F. Johnson, P. M. Hui, *Physica A* **298**, 537 (2001); N.F. Johnson, P. Jefferies, P.M. Hui, *Financial Market Complexity* (Oxford University Press, Oxford, 2003); N.F. Johnson et al., *Physica A* **258**, 230 (1998).
- [8] N.F. Johnson, P.M. Hui, cond-mat/0306516.
- [9] The Eulerian Trail corresponds to a particular cycle around the de Bruijn graph in which every possible transition between global information states is visited once. The de Bruijn graph represents the  $2^m$  possible global information states.

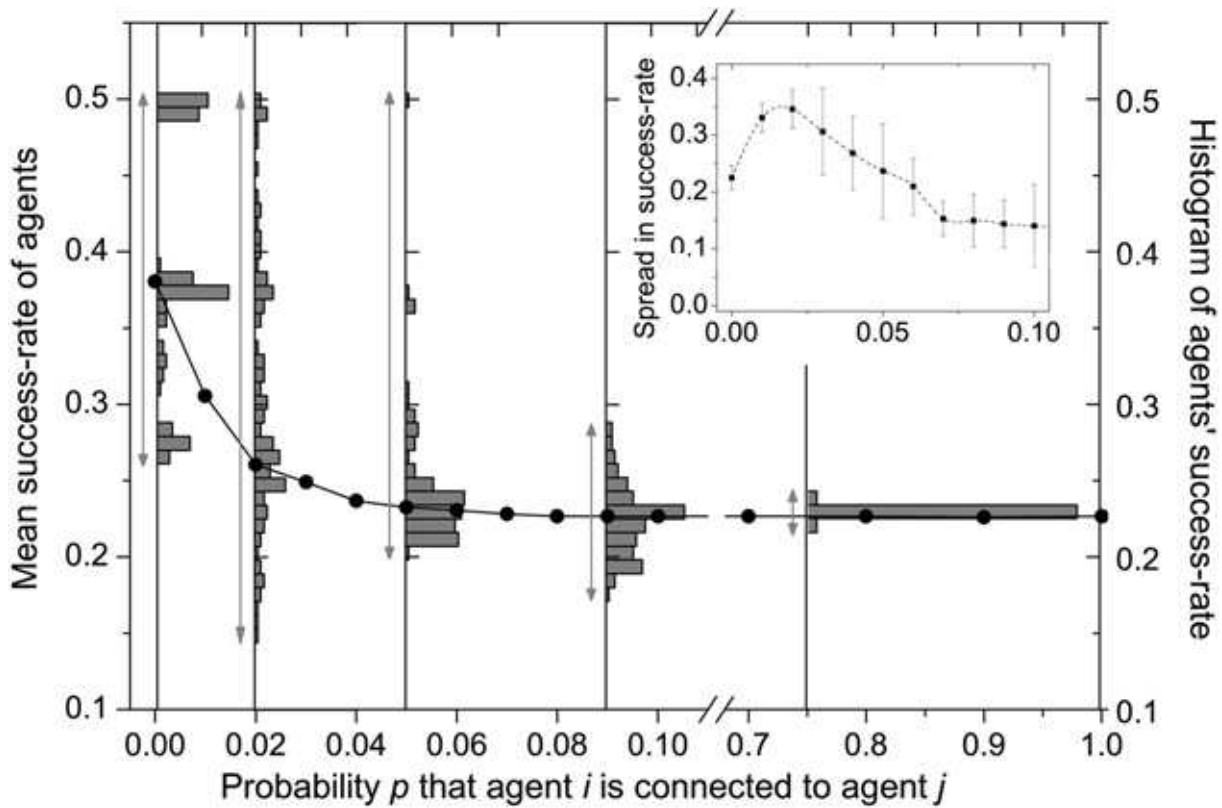


FIG. 1. Modest resource population: Solid line (left axis) shows numerically-obtained mean success-rate per agent, as a function of the probability  $p$  that agent  $i$  is connected to agent  $j$ . Right axis: typical histograms of agents' success-rate in a typical run of  $10^5$  timesteps.  $N = 101$ ,  $S = 2$ ,  $m = 1$  and  $L = 50$ . Inset: spread in success-rate as a function of  $p$ . Error bars obtained from 20 separate runs.

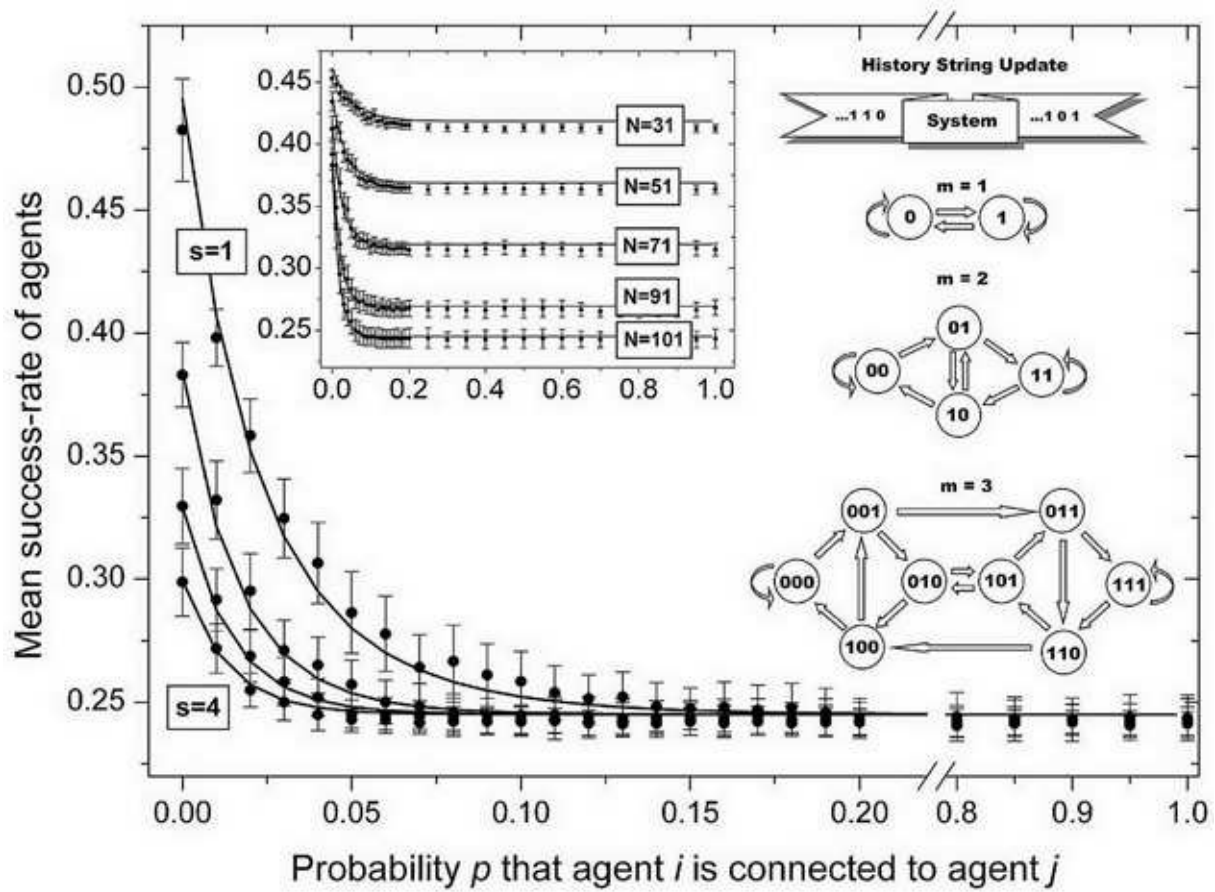


FIG. 2. Solid lines show analytic Crowd-Anticrowd theory for mean success-rate per agent in a modest resource population, for  $S = 1, 2, 3, 4$ . Data-points are numerical results.  $m = 1$ ,  $N = 101$ ,  $L = 50$ . Inset:  $S = 2$ , various  $N$  values. Right: Eulerian Trails [9] (i.e. high  $p$  attractor) for  $m = 1, 2, 3$ .

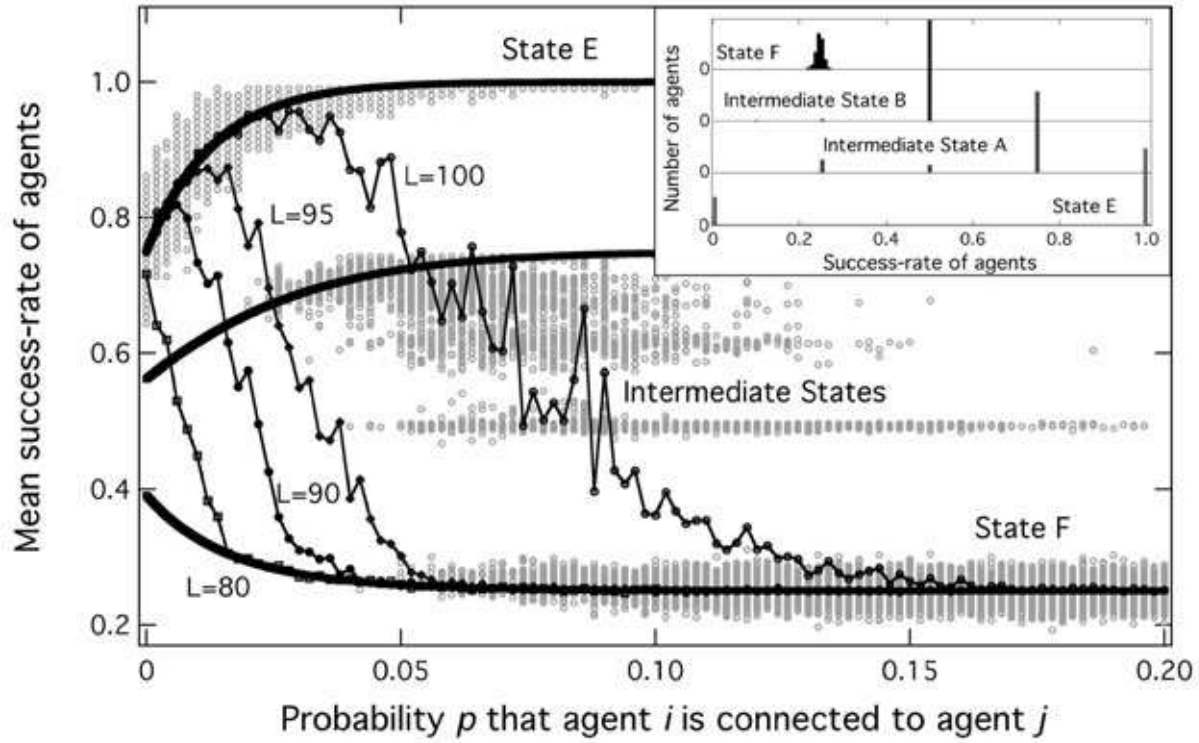


FIG. 3. Higher-resource population: Thin solid lines: numerically-obtained mean success-rate per agent as a function of  $p$ , at resource levels  $L = 80, 90, 95, 100$ . Results averaged over 200 runs of  $10^5$  timesteps, with  $N = 101, S = 2, m = 1$ . Scattered circles show mean success-rate per agent for separate runs at  $L = 100$  with  $m = 1$ , as an illustration. Thick solid lines: analytical curves (Eqs. (5)-(7)) describing the three dynamical regimes. The results agree so well over some portions, that the analytical curves obscure the numerical results. Inset: histograms of typical success-rate distribution, for  $L = 100, m = 1$ .

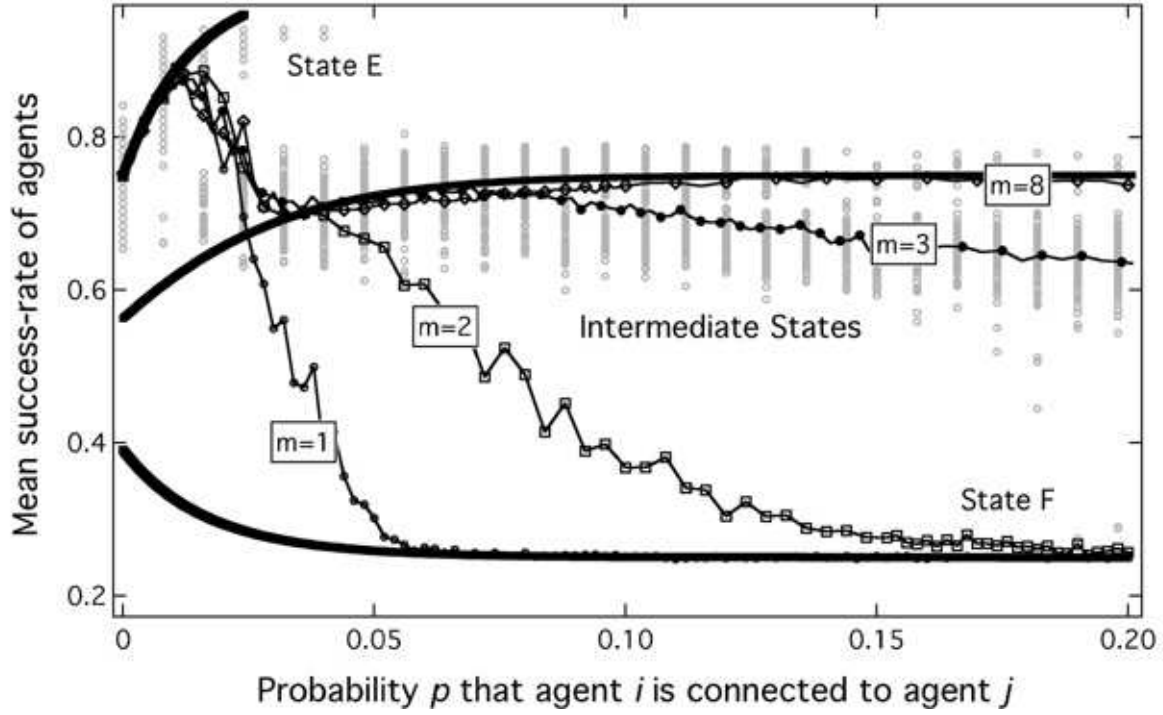


FIG. 4. High-resource population: Thin solid lines: numerically-obtained mean success-rate per agent as a function of  $p$ , at various  $m$ . Results averaged over 200 runs of  $10^5$  timesteps, with  $N = 101$ ,  $S = 2$ ,  $L = 95$ . Scattered circles show mean success-rate per agent for separate runs at  $m = 3$ . Thick solid lines: analytical curves (Eqs. (5)-(7)) describing the three dynamical regimes. The results agree so well over some portions, that the analytical curves obscure the numerical results.